

**ADDIS ABABA UNIVERSITY**  
**DEPARTMENT OF CHEMISTRY**  
**GRADUATE PROGRAM**



**Investigation of Rotational Barrier in Nicotinamide and Picolinamide  
Using Temperature-Dependent  $^1\text{H}$  NMR Spectra**

By

Ali Mohammed Sualih

Advisors: Dr. Mesfin Redi

Mr. Yisak Tsegazab

May, 2018.

# **Investigation of Rotational Barrier in Nicotinamide and Picolinamide Using Temperature-Dependent $^1\text{H}$ NMR Spectra**

Ali Mohammed Sualih

A Thesis Submitted to  
The Department of Chemistry

Presented in Partial Fulfilment of the Requirement for the Degree of Master of  
Science in Chemistry (Physical Chemistry)

Addis Ababa University

Addis Ababa, Ethiopia

May, 2018.

**ADDIS ABABA UNIVERSITY**  
**DEPARTMENT OF CHEMISTRY**  
**GRADUATE PROGRAM**

This is to certify that the thesis prepared by Ali Mohammed Sualih entitled “*Investigation of Rotational Barrier in Nicotinamide and Picolinamide Using Temperature-Dependent <sup>1</sup>H NMR Spectra*” submitted in partial fulfilment of the requirements of the degree of Master of Science in chemistry (physical chemistry) compiles with regulation of the university and meets the accepted standards with respect to originality and quality.

Approved by examining committee

Examiner: Dr. Ahmed Mustofa signature \_\_\_\_\_ date \_\_\_\_\_

Examiner: Dr. Taye Beyne signature \_\_\_\_\_ date \_\_\_\_\_

Advisor: Dr. Mesfin Redi signature \_\_\_\_\_ date \_\_\_\_\_

---

Chair of Department or Graduate Program Coordinator

## Abstract

Investigation of Rotational Barrier in Nicotinamide and Picolinamide Using Temperature-Dependent  $^1\text{H}$  NMR Spectra

Ali Mohammed Sualih

Addis Ababa University, 2018

Rotational barrier in nicotinamide and picolinamide have been investigated employing temperature-dependent proton nuclear magnetic resonance ( $^1\text{H}$  NMR) spectrometry. In nicotinamide and picolinamide the two protons on the nitrogen appeared at different chemical shift positions revealing that they are magnetically non-equivalent.

In the experiments, nicotinamide showed two distinct peaks corresponding to the amine group of the amide molecule, and the peak separation decreased as a function of temperature indicating a rotational barrier about the amide bond. The coalescence of the two peaks was observed at 328 K. Using through line shape analysis of the temperature dependent spectra; a rotational barrier of  $17.9 \text{ kcal mol}^{-1}$  was calculated. Interestingly the opposite temperature dependence of the peak separation was observed in picolinamide in which the separation increased as the temperature was increased and no convergence was observed in the temperature ranges the experiments were conducted. The observed behaviour clearly demonstrates that the splitting of the peaks cannot be attributed to the rotational barrier about the C–N bond rather it suggests that the two peaks originate from two different chromophores (O–H and =N–H chromophores) resulting from a tautomeric equilibrium.

Key words:  $^1\text{H}$  NMR, nicotinamide, picolinamide, rotational barrier, rate constant,

## **Acknowledgement**

I take this opportunity to express my deepest appreciation to Dr. Mesfin Redi, who not only served as my advisor, providing valuable and countless resource, insight, but also constantly gave me support, encouragement, and reassurance. I am grateful to my co-advisor Yisak Tsegazab (Msc.) for his inspirational and timely support, technical expertise and acuity throughout the duration of the project. I am grateful to Dr. Yonas Chebude for his genuine encouragement, and support in the spectra of different samples, during the entire work. Special thanks are given to PhD student Kassahun Dejene, and my partners Msc. students, Haile Abegaz, Basznew Dilnessa, Abdu Mohammed, Mubarek Hussain, and Amin Abdullahi for sharing their knowledge resources with me.

Last, but not least, I would like to express profound gratitude to my mother, and my wife Zebiba Mohammed.

# Table of Contents

Abstract.....	i
Acknowledgement.....	ii
List of Figures .....	v
List of tables.....	vi
List of Abbreviations.....	vii
1 Introduction.....	1
2 Theoretical aspect.....	3
2.1 Amides.....	3
2.1.1 Structure and Classification of Amide .....	3
2.2 Fundamentals of spectroscopy.....	5
2.3 Interaction of electromagnetic radiation with molecular system.....	6
2.3.1 Macroscopic polarization .....	8
2.3.2 Microscopic polarization.....	9
2.3.3 Real and imaginary parts of susceptibilities (Kramers-Kronnig relations)	9
2.3.4 Kramers–Kronig relations with Kerr susceptibility $\chi^{(3)}$ .....	10
2.4 NMR spectroscopy.....	12
2.4.1 Properties of nuclei .....	13
2.4.2 Spin-spin splitting in proton NMR.....	15
2.4.3 Chemical Shift .....	16
2.4.4 NMR Data Processing.....	16
2.4.5 The Fourier Transform (FT) NMR .....	17
2.5 Temperature dependent on rotational barrier of amide bond .....	18
2.5.1 Evaluation of rate exchange constant (k).....	18
2.5.2 Approximate methods for evaluation of rate constant (k).....	20

2.6	Temperature dependent of the exchange rate to evaluate thermodynamic quantities .....	22
3	Objectives .....	24
3.1	General objective .....	24
3.2	Specific objectives .....	24
4	Experimental part .....	25
4.1	Materials .....	25
4.2	Methods and procedures .....	25
4.2.1	Proton NMR measurements .....	25
5	Results and Discussion .....	27
5.1	<sup>1</sup> H NMR Result Nicotinamide .....	27
5.2	Determination of Kinetic Parameter for Nicotinamide .....	28
5.2.1	Rate exchange constant (k) .....	28
5.2.2	Activation energy .....	30
5.3	Determination of Thermodynamic Parameters for Nicotinamide .....	30
5.3.1	Enthalpy change, entropy change, and free energy change .....	30
5.4	The <sup>1</sup> H NMR Result for Picolinamide .....	32
6	Conclusion .....	36
7	References .....	37
8	Appendices .....	39

## List of Figures

Figure 1. General structure of amides. ....	3
Figure 2. General structure and classification of amides .....	3
Figure 3. The structure of nicotinamide and picolinamide.....	4
Figure 4. Resonance stabilization of nicotinamide. ....	4
Figure 5. Rotation about the amide bond leads to exchange the two protons on nitrogen.....	4
Figure 6. The electromagnetic spectrum (the scale is logarithmic)[9].....	5
Figure 7. The imaginary and the real part of NMR spectrum of an amide .....	12
Figure 8. Energy levels for a nucleus with spin quantum number [15]. ....	14
Figure 9. The free induction decay (FID) is on the left and its Fourier transform (usual frequency spectrum) is on the right of an amide.....	17
Figure 10. Effect of exchange of chemically equivalent nuclei on NMR lineshapes [17]. ....	20
Figure 11. Effect of temperature on lineshape for the two protons on nitrogen in nicotinamide in ACN.....	27
Figure 12. the proton NMR spectra of picolinamide (b) in acetonitrile and (c) in benzene solvents as a function of temperature. ....	32
Figure 13. Plot of frequency versus temperature of nicotinamide in acetonitrile.....	33
Figure 14. plot of frequency versus temperature of picolinamide in benzene.....	33
Figure 15. plot of frequency versus temperature of picolinamide in Acetonitrile.....	34
Figure 16. The chemical shifts of nicotinamide at different temperatures.....	34
Figure 17. the chemical shifts of the tautomeric form of picolinamide .....	35
Figure 18. $\ln k$ Vs $1/T$ for nicotinamide .....	39
Figure 19. $\ln(k/T)$ Vs $1/T$ for nicotinamide. ....	39

## List of tables

Table 1. Change of peak separation and peak widths at half height with various temperatures of nicotinamide.....	28
Table 2. Typical value for $k_{rate}$ for nicotinamide .....	29
Table 3. Comparison of Experimental energies for rotational barrier of nicotinamide .....	31

## List of Abbreviations

$^1\text{H}$  NMR ..... Proton nuclear magnetic resonance

$\text{C}_6\text{D}_6$  ..... Deuterated benzene

C-N ..... Carbon Nitrogen bond

CO ..... Carbonyl bond

MHz ..... Mega Hertz

TMS ..... Tetramethylsilane

NLO ..... Non-linear optics

Eq. .... Equation

$K_{\text{rate}}$  ..... Exchange rate constant

$E_a$  ..... Activation Energy

$\Delta H$  ..... Enthalpy Change

$\Delta G$  ..... Free Energy Change

$\Delta S$  ..... Entropy Change

K ..... Kelvin

# 1 Introduction

Amides are organic molecules which have a functional group that consists of a C=O (carbonyl) bond to a nitrogen atom. Understanding the structure of the amides is fundamental for modelling and predicting their behaviour in larger molecules, such as proteins which plays essential roles in biological processes, functioning as structural supporters, catalysts, signal transmitters, and so on. Their biological functions are determined by their three-dimensional structures, which undergo constant motions over a wide range time and length scale [1]. In addition amides are interesting functional compounds which play great role in organic synthesis and pharmaceutical industries.

Amides can be classified as 1<sup>st</sup>, 2<sup>nd</sup>, and 3<sup>rd</sup>, order based on the number of hydrogen atom on the nitrogen atom of the amide. An important aspect the amide in the C-N bond has a partial double bond nature that results from the resonance of the non-bonding electron of the nitrogen, N, and the carbonyl, CO, group of the amides. This leads planarization of the amide molecule around -N-CO moiety [2]. Because of the partial double bond characteristic nature of the amide, there will be rotational barrier about the amide bond. Ramiro Quintanilla-Licea, et al, [3], suggests that the rotational barrier of C-N partial double bond of formamide the two protons on the nitrogen atom are non-equivalent due to the mentioned hindered rotation about the C-N bond. In the corresponding <sup>1</sup>H NMR spectrum two protons on the nitrogen atom signals are found at  $\delta = 7.21$  and  $7.48$  ppm, together with a singlet at  $\delta = 8.21$  for the formyl proton. Therefore this leads to the difference in chemical shift absorption of the two protons on nitrogen of the amide [3].

Experimentally, the structure and bonding form of amides can be analyzed using NMR spectroscopic techniques. NMR is extensively used to determine the environment in which the specific atoms exist.

Hence in this experiment the rotational barrier of nicotinamide and picolinamide are investigated using dynamic proton NMR spectroscopy.

The beauty of this method is due to the characteristic period of the NMR measurements, a range of the reaction rates usually encountered in the laboratory is

easy accessible ( $10^{-1}$ - $10^{-5}$  s<sup>-1</sup>). In addition, the exchange rate in rotational barriers can be studied by this method.

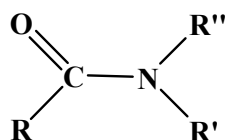
the effect of exchange at several temperatures are investigated via proton NMR spectra So that at low temperatures the exchange is slow which is the rate constant is much less than the chemical shift change, this implies that the spectrum consists of two sharp singlets. At high temperature the exchange is fast which is the rate exchange constant is greater than the chemical shift change, i.e., there is a rapid rotation about the amide bond then the magnetic non-equivalence disappears, therefore only one peak can be observed in the proton NMR spectra. There is also an intermediate temperature range over which the spectrum consists of two significantly broadened overlapping lines, which are said to be coalescence temperature.

The kinetic and thermodynamic parameters for rotation of amide bond have been evaluated through the temperature dependant proton NMR spectrometry.

## 2 Theoretical aspect

### 2.1 Amides

Amides are organic molecules, amide bond formation is a fundamentally important reaction in organic synthesis, in pharmaceutical industries, besides amide bond plays a major role in composition of biological system such as proteins, nucleic acids; Proteins are large molecules which contain repeating amide units. They are formed when carboxylic acid group of one amino acid condenses with the amino group of another to form an amide linkage, also known as a peptide bond [4]. Therefore an amide has a functional groups that consists of a carbonyl, CO, to nitrogen, N, of the amide.

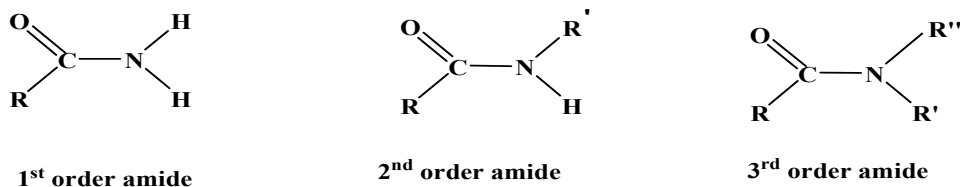


Where R , R' and R'' alkyl or aryl or hydrogen.

Figure 1. General structure of amides.

#### 2.1.1 Structure and Classification of Amide

Amides can be classified as 1<sup>st</sup> order, 2<sup>nd</sup> order, and 3<sup>rd</sup> order, depending on the substituent on nitrogen as shown in figure 2.



Where R is hydrogen, alkyl, or aryl group, and R', and R'' are alkyl or aryl group.

Figure 2. General structure and classification of amides

Amides have different types of hydrogen: hydrogen on the carbonyl side, hydrogen attached to the carbon atom on the alkyl (or aryl) group on the carbonyl side, which is called  $\alpha$ -hydrogen, hydrogen those attached to the nitrogen atom of the amid.

The conformation of the amide bond plays an important role in determining the backbone structure of the proteins and related compounds. Most of the properties of amides are readily rationalized by postulating amide resonance structures,[5]. Since

Here we are interested in 1<sup>st</sup> order amide which are nicotinamide and picolinamide (figure 3)

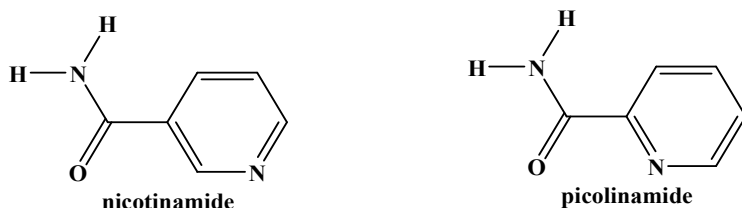


Figure 3. The structure of nicotinamide and picolinamide.

Amides are stable molecules. The reason for stability of amides is the resonance interaction of the non bonding electron of the nitrogen and the  $\pi$ -bond in carbonyl, CO, group. This electron delocalization in amides (Figure 4) causes the O-C-N bond to have double bond character. This in turn makes the energy required to rotate about that C-N partial double bond of amides (figure 5) significantly higher than that for rotation about C-N single bonds and its rotation is fixed [6].

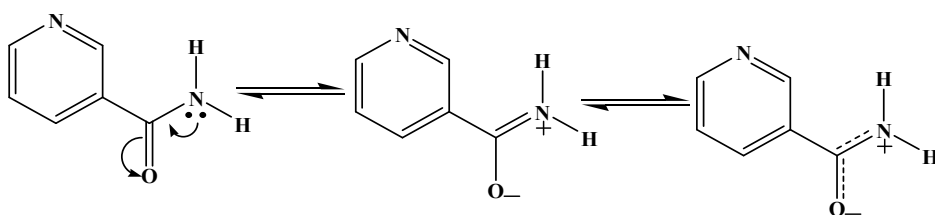


Figure 4. Resonance stabilization of nicotinamide.

The protons ( $H_a$  and  $H_b$ ) on the nitrogen of the amide (figure 5) have different chemical environments, i.e., magnetically non-equivalent, so therefore they have distinct  $^1\text{H}$  NMR signals. And of course these signals are temperature dependent.

The resulting dynamic NMR spectra are providing kinetic and thermodynamic parameters through variable temperature NMR experiments

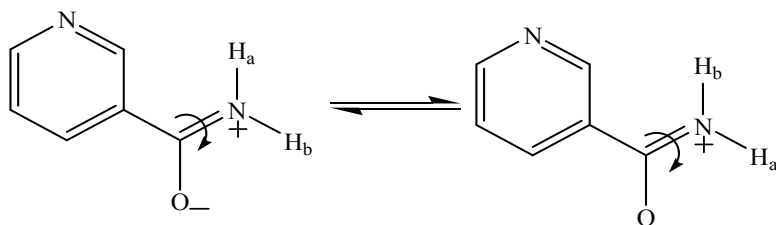


Figure 5. Rotation about the amide bond leads to exchange the two protons on nitrogen.

## 2.2 Fundamentals of spectroscopy

Spectroscopy is the study of the quantized interaction of electromagnetic energy with matter. In organic chemistry, typically deal with molecular spectroscopy, i.e. the spectroscopy of atoms that are bound together in molecules [7]. Molecular spectroscopy is a means of probing molecules and by absorption of electromagnetic radiation. The absorbed electromagnetic radiation results in transitions between eigenstates of a molecule. The type of eigenstates involved in a transition depends on the energy of the radiation absorbed. Figure 1 shows an electromagnetic spectrum along with the relative energies, wavelengths, and frequencies associated with each type of radiation. The absorbed ultraviolet and visible radiation generally results in transitions amongst electronic eigenstates, the absorbed infrared radiation results in changes in vibrational eigenstates, and the absorbed microwave radiation results in changes in rotational eigenstates [8]. The specific wavelengths of radiation that are absorbed in each region of electromagnetic spectrum depend on the energy difference between the eigenstates of a molecule. The absorbed radiation in a spectrum provides information on the energy differences amongst various eigenstates of a molecule; however, it does not provide any information on the actual eigenstates involved in the transitions. Quantum mechanics is needed in order to analyze a spectrum in terms of assigning a spectrum to a specific transition in eigenstates of a molecule.

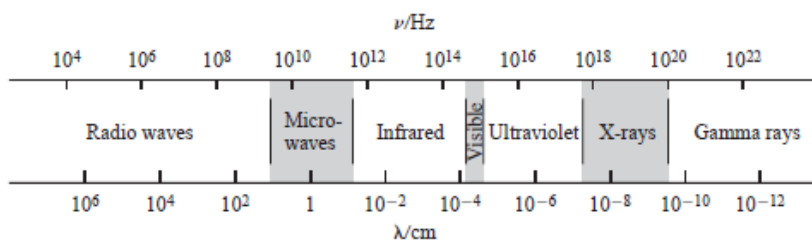


Figure 6. The electromagnetic spectrum (the scale is logarithmic)[9]

The energy of a photon of the electromagnetic radiation is directly proportional to its frequency  $\nu$ , and is inversely proportional to its wavelength  $\lambda$ .

$$E_{\text{photon}} = h\nu = \frac{hc}{\lambda} \quad (1)$$

## 2.3 Interaction of electromagnetic radiation with molecular system

All macroscopic aspects of the static and dynamics of the electromagnetic field in the presence of material media are described by Maxwell's equations [10, 14].

$$\nabla \cdot \mathbf{D}(r,t) = \rho(r,t) \quad \text{Gauss's Law} \quad (2)$$

$$\nabla \cdot \mathbf{B}(r,t) = 0 \quad (3)$$

$$\nabla \times \mathbf{E}(r,t) = -\frac{\partial}{\partial t} \mathbf{B}(r,t) \quad \text{Faraday's Law} \quad (4)$$

$$\nabla \times \mathbf{H}(r,t) = \frac{\partial}{\partial t} \mathbf{D}(r,t) + \mathbf{J}(r,t) \quad \text{Ampere's Law} \quad (5)$$

For a given position  $\mathbf{r}$  (m) and a time  $t$  (s) the Maxwell's equations couple the dielectric displacement vector  $\mathbf{D}$  ( $\text{Cm}^{-2}$ ). The charge density  $\rho$  ( $\text{C m}^{-3}$ ), the magnetic induction vector  $\mathbf{B}$  (T:  $\text{T}=\text{s m}^{-2}$ ), the electric field strength  $\mathbf{E}$  ( $\text{V m}^{-1}$ ), the magnitude field strength  $\mathbf{H}$  ( $\text{A m}^{-1}$ ) and the total current density  $\mathbf{J}$  ( $\text{A m}^{-2}$ )

The response of the medium to the electric and magnetic fields may be expressed by the so called constructive or material equations:

$$\mathbf{D}(\mathbf{r},t) = \varepsilon_0 \mathbf{E}(\mathbf{r},t) + \mathbf{P}(\mathbf{r},t) \quad (6)$$

$$\mathbf{B}(\mathbf{r},t) = \mu_0 \mathbf{H}(\mathbf{r},t) + \mu_0 \mathbf{M}(\mathbf{r},t) \quad (7)$$

$\mathbf{P}$  is the dielectric polarization vector ( $\text{C m}^{-2}$ ) induced by the electric field,  $\mathbf{M}$  is the magnetization vector ( $\text{A m}^{-1}$ ) induced by the magnetic field,  $\varepsilon_0$  is the vacuum permittivity ( $\varepsilon_0 = 8.85419 \times 10^{-12} \text{ CV}^{-1} \text{ m}^{-1}$ ) and is the vacuum permeability ( $\mu_0 = 4 \pi \times 10^{-7} \text{ C}^{-1} \text{ m}^{-1}$ ). Assume the media do not contain macroscopic charge and current density, hence  $\rho = 0$  and  $J = 0$ , and they are not magnetized, so that  $\mathbf{M}=0$ . Then Maxwell's equations and the constitutive relations may be combined to yield the following coupled partial differential equation between the electric field  $\mathbf{E}$  and the dielectric polarization  $\mathbf{P}$ .

$$\nabla \times \nabla \times \mathbf{E}(\mathbf{r}, t) = -\mu_0 \frac{\partial^2}{\partial t^2} \{ \epsilon_0 \mathbf{E}(\mathbf{r}, t) + \mathbf{P}(\mathbf{r}, t) \} \quad (8)$$

The solution of the above equation for the case of linear optics where constitutive relation defines  $\mathbf{P}$  as a linear function of the electric field. Optically linear medium are characterized by a linear response of the medium to the electric field. Considering electric field at position  $\mathbf{r}$  which varies sinusoidally with time where a macroscopic field  $\mathbf{E}(t)$  i.e.,  $\mathbf{E}(t) = \mathbf{E}_0 \cos(\omega t)$ . in the electric dipole approximation, the dielectric polarization  $\mathbf{P}(t)$  is created by local response in the medium[11,14].

$$\mathbf{P}(t) = \epsilon_0 \chi^{(1)} \cdot \mathbf{E}_0 \cos(\omega t) \quad (9)$$

Where the linear susceptibility  $\chi^{(1)}$  is a tensor quantity characteristic of the first order linear response of the medium is frequency-dependent. The argument in parentheses describes the nature of this dependence. Two waves interact with each other through the medium. The frequency of the resulting wave is stated first, then the frequency of the incident wave(s). In general,  $\chi^{(1)}$  is a second-rank tensor, that is, a 3x3 matrix.

For optically linear medium  $\nabla \cdot \mathbf{E} = 0$  and applying the identity:  $\nabla \times \nabla \times \mathbf{E} = \nabla(\nabla \cdot \mathbf{E}) - \Delta \mathbf{E}$  the electric field in vacuum can be written

$$\mathbf{E}(\mathbf{r}, t) = \mathbf{E}_0 e^{i(\mathbf{k} \cdot \mathbf{r} - \omega t)} \quad (10)$$

For a wave propagation in +z-direction in a weakly absorbing medium:

$$\mathbf{E}(z, t) = \mathbf{E}_0 \exp\left(-\frac{1}{2} \alpha z\right) \cos(\omega t - \kappa z) \quad (11)$$

Where  $\alpha$  is the natural absorption coefficient and  $k$ , ( $k = 2\pi n / \lambda$ ), is the magnitude of the wave vector. Both  $\alpha$  and  $n$  represent the linear response of the medium and linked to the imaginary and real part of  $\chi^{(1)}$ .

$$\alpha = \frac{\omega \text{Im}\{\chi^{(1)}\}}{c_0} \quad (12)$$

$$n^2 = 1 + \text{Re}\{\chi^{(1)}\} \quad (13)$$

### 2.3.1 Macroscopic polarization

The electric  $n^{\text{th}}$ -order susceptibilities,  $(\chi^n)$ , describe the polarization of a macroscopic portion of matter (for example, a dielectric medium) in the presence of an electric field.

Considering an experimental situation where a macroscopic (or Maxwell) field  $\mathbf{E}(t)$  is generated in a medium by the superposition of a static and one optical component, that is

$$\mathbf{E}(t) = \mathbf{E}^0 + \mathbf{E}^\omega \cos(\omega t) \quad (14)$$

Where  $\mathbf{E}^0$  is the static amplitude, and  $\mathbf{E}^\omega$  is the optical field. The response of the medium can be represented by the dielectric polarization vector (dipole moment per unit volume)  $\mathbf{P}(t)$ , which, in terms of Fourier components, yields

$$\mathbf{P}(t) = P^0 + P^\omega \cos(\omega t) + P^{2\omega} \cos(2\omega t) + \dots \quad (15)$$

Each Fourier amplitudes the  $P^0, P^\omega, P^{2\omega}$  can be expanded as a power series with respect to the electric field, so that

$$\begin{aligned} P^0 &= \chi^{(0)} + \chi^{(1)}(0;0) \cdot E^0 + \chi^{(2)}(0;0,0) : E^0 E^0 + \\ &\quad \frac{1}{2} \chi^{(2)}(0;-\omega, \omega) E^\omega E^\omega + \chi^{(3)}(0;0,0,0) : E^0 E^0 E^0 + \dots \\ P^\omega &= \chi^{(1)}(-\omega, \omega) \cdot E^\omega + 2\chi^{(2)}(-\omega, \omega, 0) : E^\omega E^0 + 3\chi^{(3)}(-\omega, \omega, 0, 0) : E^\omega E^0 E^0 + \dots \\ P^{2\omega} &= \frac{1}{2} \chi^{(2)}(-2\omega, \omega, \omega) : E^\omega E^\omega + \frac{1}{3} \chi^{(3)}(-2\omega, \omega, \omega, 0) : E^\omega E^\omega E^0 + \dots \end{aligned} \quad (16)$$

Where the argument in the parentheses of the susceptibility tensor,  $\chi^{(n)}$ , describes the nature of the frequency dependence at a given order; in all cases, the frequency of the resulting wave is stated first, followed by the frequency of the incident interacting waves (two in a first-order process, three in the second-order analogue, and four in the third-order case)[12,14].

### 2.3.2 Microscopic polarization

The molar polarizabilities can be interpreted microscopically in terms of the NLO response of a molecule to an electric field [12, 13]. Through linear and non-linear optical processes in the medium, the field of Eq. (13) will give rise to Fourier components  $E^{L\Omega}$  of the local electric field  $E^L$  at frequencies  $\Omega = 0, \omega, 2\omega, \dots$

$$E^L(t) = \sum_{\Omega=0,\omega,2\omega} E^{L\Omega} \cos(\Omega t) \quad (17)$$

And the total dipole moment  $P(t)$  of the solute molecule will exhibit a time dependence of the general form Eq. (15)

For the derivation of the local-field corrections and effective polarizabilities below, we consider the Fourier amplitudes of  $P(t)$ .

$$P^0 = \mu^0 + \alpha(0;0) \cdot E^{L0} + \frac{1}{2} \beta(0;0,0) : E^{L0} E^{L0} + \frac{1}{4} \beta(0;-\omega,\omega) : E^{L\omega} E^{L\omega} + \dots$$

$$P^\omega = \alpha(-\omega;\omega) \cdot E^{L\omega} + \beta(-\omega;\omega,0) : E^{L\omega} E^{L0} + \frac{1}{2} \gamma(-\omega;\omega,0,0) : E^{L\omega} E^{L0} E^{L0} \\ + \frac{1}{8} \gamma(-\omega;-\omega,\omega,\omega) : E^{L\omega} E^{L\omega} E^{L\omega} + \dots$$

$$P^{2\omega} = \alpha(-2\omega;2\omega) \cdot E^{L2\omega} + \frac{1}{4} \beta(-2\omega;\omega,\omega) : E^{L\omega} E^{L\omega} + \frac{1}{4} \gamma(-2\omega;\omega,\omega,0) : E^{L\omega} E^{L\omega} E^{L0} \\ + \frac{1}{4} \delta(-2\omega;\omega,\omega,0,0) : E^{L\omega} E^{L\omega} E^{L0} E^{L0} + \dots \quad (18)$$

Where  $\mu^0$  is the permanent dipole moment and  $\alpha, \beta, \gamma, \delta, \dots$  are (hyper) polarizabilities of the isolated solute molecule [13, 14].

### 2.3.3 Real and imaginary parts of susceptibilities (Kramers-Kronig relations)

For the case of real susceptibilities Eq. (16) is given. However, it has to be treated as complex quantities if the frequency is close to or within the region of an optical transition in the medium. From linear optics in Eq.(12) the imaginary part of the first order susceptibility,  $\chi^{(1)}$  was related to the absorption coefficient,  $\alpha^\omega$ , of the medium. And the real part of the first order susceptibility,  $\chi^{(1)}$  was related to the refractive

index,  $n^0$  of the medium (Eq. (13)). The real and imaginary parts of susceptibility are in certain cases coupled through Kramers-Kronig relations [14] written as.

$$\text{Re}\{\chi(\omega')\} = \frac{2}{\pi} P \int_0^{+\infty} d\omega \frac{\omega \text{Im}\{\chi(\omega)\}}{\omega^2 - (\omega')^2} \quad (19)$$

### 2.3.4 Kramers–Kronig relations with Kerr susceptibility $\chi^{(3)}$

The quadratic effect of an externally applied field on the refractive index,  $n$ , is described by the third-order susceptibility  $\chi^{(3)}$  (Kerr susceptibility). The two independent components  $\chi_{zzzz}^{(3)}$  and  $\chi_{zzxx}^{(3)}$  can be interpreted in terms of molar polarizabilities. The results with only one significant component  $\beta_{zzz}^{(3)}$  of the second-order polarizability are expressed in Eq.(20)and Eq.(21).

$$\zeta_{zzzz}^3(-\omega; \omega, 0, 0) = \frac{N_A}{90} \left[ \frac{4}{3K^2T^2} (\bar{\mu}_z^g)^2 \delta\bar{\alpha}_z(-\omega; \omega) + \frac{6}{KT} \bar{\mu}_z^g \bar{\beta}_{zzz}(-\omega; \omega, 0) \right] \quad (20)$$

$$\zeta_{zzxx}^3 = \frac{N_A}{90} \left[ \frac{-2}{3K^2T^2} (\bar{\mu}_z^g)^2 \delta\bar{\alpha}_z + \frac{2}{KT} \bar{\mu}_z^g \bar{\beta}_{zzz} \right] \quad (21)$$

In the region of an absorption band of the medium, the first-order susceptibility  $\chi^{(1)}$  has to be treated as a complex quantity, the real and imaginary part determining the refractive index (13) and the absorption coefficient of the medium (12), respectively. The imaginary part of the molar first-order polarizabilities [14] is written as

$$\text{Im}\left[\zeta^{(1)}\right] = \frac{N_A}{3} \text{Tr}\left[\text{Im}(\bar{\alpha})\right] = \ln(10) c_0 \varepsilon_0 n^0 \frac{\varepsilon(\omega)}{\omega} \quad (22)$$

Where  $\varepsilon(\omega)$  is the molar decadic absorption coefficient of the solute determined by Beer's law. The factor  $\ln(10)$ , natural logarithm of 10, is due to the conversion between the natural absorption coefficient (Eq.12) and the decadic coefficient  $\varepsilon$ . The real and the imaginary part of  $\zeta^{(1)}$  and  $\chi^{(1)}$  are related by a Kramers-Kronig transformation (Eq.19). Integration of the absorption spectrum over an isolated transition  $|a\rangle \leftarrow |g\rangle$  yields the magnitude of the transition dipole  $\mu^{ag}$  is written as

$$\int_{band} \frac{\varepsilon(\omega)}{\omega} d\omega = \frac{2\pi^2 N_A}{3 \ln(10) h c_0 \varepsilon_0} |\mu^{ag}|^2 \quad (23)$$

Considering electromism (electro-optical absorption measurements (EOAM)) of the solution the imaginary part of the third-order susceptibility  $[\text{Im}(\chi^3)]$ . The technique is used to gain information on molecular ground and excited state dipole moments, as well as the magnitudes and direction of the corresponding transition dipoles.

The quadratic effect of an externally applied field,  $\mathbf{E}^0$ , on the absorption coefficient is described by the imaginary part of the third-order susceptibility  $\chi^{(3)}$ .  $\mathbf{E}^0$  influences the molar decadic absorption coefficient of the solute. The absorption coefficient in the presence of the field  $\varepsilon^E$  is a quadratic function of the applied field strength.

$$\varepsilon^E(\omega) = \varepsilon(\omega) \left[ 1 + L(\omega) (\mathbf{E}^0)^2 + \dots \right] \quad (24)$$

Where the quantity L is a measure of the relative change of  $\varepsilon$  induced by  $\mathbf{E}^0$ . L depends on the frequency as well as on angle between the polarization vector of the incident light and the applied field. A detailed microscopic interpretation of the electrochromic effect in liquid solutions has been given [14]. The results are written here with those of the molar polarizabilities introduced above. The relation between the traditional quantity L and the molar polarizabilities introduced above is found to be.

$$\text{Im} \left\{ \zeta^{(3)}(-\omega; \omega, 0, 0) \right\} = \frac{1}{3} \ln(10) c_0 \varepsilon_0 n^\omega \frac{L(\omega) \varepsilon(\omega)}{\omega} = \frac{1}{3} L(\omega) \text{Im} \left\{ \zeta^{(1)}(-\omega; \omega) \right\} \quad (25)$$

For an isolated electronic transition between a ground state  $|g\rangle$  and an excited state  $|a\rangle$ , the molar polarizabilities can be represented by Eq. (26) and Eq.(27).

$$\text{Im} \left\{ \zeta_{zzzz}^{(3)} \right\} = \frac{N_A}{90 K^2 T^2} \left[ \begin{aligned} & 2 \left[ 3(m \bar{\mu}^g) - (\bar{\mu}^g)^2 \right] \text{Im} \left\{ \zeta^{(1)} \right\} + \\ & \frac{6}{KT} \left[ 2(\bar{\mu}^g \Delta \bar{\mu}^{ag}) + 2(m \bar{\mu}^g)(m \Delta \bar{\mu}^{ag}) \right] \frac{1}{\hbar} \frac{d}{d\omega} \text{Im} \left\{ \zeta^{(1)} \right\} \end{aligned} \right] \quad (26)$$

$$\text{Im}\{\zeta_{zzxx}^{(3)}\} = \frac{N_A}{90K^2T^2} \left[ \begin{aligned} & -\left[3(m\bar{\mu}^g) - (\bar{\mu}^g)^2\right] \text{Im}\{\zeta^{(1)}\} + \\ & \frac{6}{KT} \left[ 2(\bar{\mu}^g \cdot \Delta\bar{\mu}^{ag}) - (m\bar{\mu}^g)(m\Delta\bar{\mu}^{ag}) \right] \frac{1}{\hbar} \frac{d}{d\omega} \text{Im}\{\zeta^{(1)}\} \end{aligned} \right] \quad (27)$$

A number of usually small terms related to the ground state polarizability, the transition polarizability and the square of the dipole difference have been neglected in Eq.(26) and Eq.(27). Complete expressions have been given. Neglecting changes of the polarizability upon excitation, the effective dipole difference in solution in Eq. (26), and Eq.(27) is given by

$$\Delta\bar{\mu}^{ag} = f^{C_o} F^{R_o} \Delta\mu^{ag} \quad (28)$$

The real and imaginary parts of  $\zeta^{(3)}$  and  $\chi^{(3)}$  are related by a Kramers-Kronig transformation [14] given in Eq. (19).

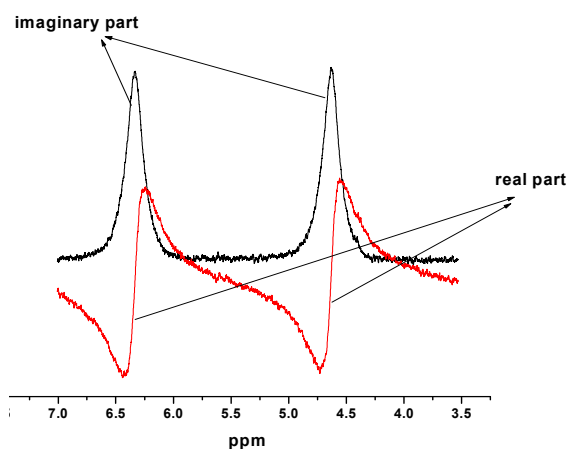


Figure 7. The imaginary and the real part of NMR spectrum of an amide

## 2.4 NMR spectroscopy

NMR spectroscopy is one of the most powerful techniques available for studying the structure of molecules. It is considered as absorption spectroscopy, thereby involves the absorption of radio waves by the nuclei of some combined atoms in a molecule that is located in a magnetic field. Radio waves are low energy electromagnetic radiation. Their frequency is on the order of  $10^7$  Hz. The energy of radiofrequency (RF) radiation can therefore be calculated by using Eq. (1).

The quantity of energy involved in RF radiation is very small. It is too small to vibrate, rotate, or electronically excite an atom or molecule. It is great enough to

affect the nuclear spin of atoms in a molecule. As a result, spinning nuclei of some atoms in a molecule in a magnetic field can absorb RF radiation and change the direction of the spinning axis. In principle, each chemically distinct atom in a molecule will have a different absorption frequency (or resonance) if its nucleus possesses a magnetic moment. The analytical field that uses absorption of RF radiation by such nuclei in a magnetic field to provide information about a sample is NMR spectroscopy [15].

NMR is a technique that enables us to study the shape and structure of molecules. In particular, it reveals the different chemical environments of the NMR-active nuclei present in a molecule, from which we can ascertain the structure of the molecule. NMR provides information on the spatial orientation of atoms in a molecule. If we already know what types of compounds are present, NMR can provide a means of determining how much of each is in the mixture. It is thus a method for both qualitative and quantitative analyses, particularly of organic compounds. In addition, NMR is used to study chemical equilibrium, reaction kinetics, the motion of molecules, and intermolecular interactions [15].

### 2.4.1 Properties of nuclei

To understand the properties of certain nuclei in an NMR experiment, since all nuclei contain protons they are charged and we must assume that nuclei rotate about an axis and therefore have a nuclear spin, represented as  $I$ , the spin quantum number. The spin quantum number,  $I$ , is a physical property of the nucleus, which is made up of neutron and proton. The spinning of a charged body generates a magnetic moment along the axis of rotation. For a nucleus to give a signal in an NMR experiment, it must have a nonzero spin quantum number ( $I$ ) and must have a magnetic dipole moment. The number of orientations or number of magnetic quantum states is a function of the physical properties of the nuclei and is numerically equal to  $2I + 1$ , allowed spin states with integral differences ranging from  $+I$  to  $-I$ . The individual spin states fit into the sequence,  $+I, (I-1), \dots, (I+1), -I$ .

In some atoms like  $^{12}\text{C}$ ,  $^{16}\text{O}$ ,  $^{32}\text{S}$ , ... these spins are paired and cancel each other out so that the nucleus of the atom has no overall spin. However in many atoms like  $^1\text{H}$ ,  $^{13}\text{C}$ ,  $^{31}\text{P}$ ,  $^{19}\text{F}$ , ..., the nucleus has an overall spin. The following rules are used to determine the spin of a given nucleus:

If the number of neutrons and protons are both even, the nucleus has no spin. If the number of neutrons and protons is odd, then the nucleus has a half-integer spin, i.e.,  $\frac{1}{2}, \frac{3}{2}, \frac{5}{2}, \dots$ . If the number of neutrons and protons are both odd, then the nucleus has an integer spin, i.e., 1, 2, 3, ... Therefore, the NMR phenomenon is based on the fact that nuclei of atoms have magnetic properties these magnetic properties are used to give chemical information.

When a nucleus with  $I=1/2$ , such as  $^1H$  is placed in an external magnetic field, its magnetic moment lines up in one of two directions, with the applied field or against the applied field. This results in two discrete energy levels, one of higher energy than the other, as shown in Figure 8. The lower energy level is that where the magnetic moment is aligned with the field. The lower energy state is energetically more favoured than the higher energy state, so the population of the nuclei in the lower energy state will be higher than the population of the higher energy state. The difference in energy between levels is proportional to the strength of the external magnetic field [15].

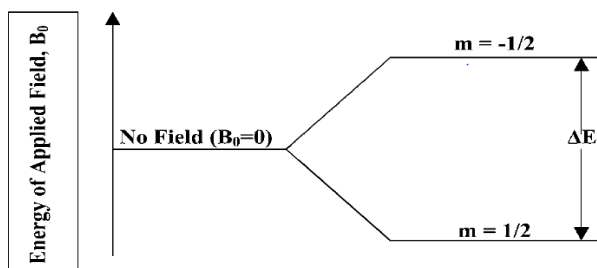


Figure 8. Energy levels for a nucleus with spin quantum number [15].

The axis of rotation also rotates in a circular manner about the external magnetic field axis, like a spinning top, as shown in Figure 8. This rotation is called precession, i.e., the particle uniformly periodic moves. The direction of precession is either with the applied field  $B_0$  or against the applied field.

So we have nuclei, in this case, protons, with two discrete energy levels. In a large sample of nuclei, more of the protons will be in the lower energy state. The basis of the NMR experiment is to cause a transition between these two states by absorption of radiation. It can be seen from Figure 8 that a transition between these two energy states can be brought about by absorption of radiation with a frequency that is equal to  $\Delta E$  according to the relationship  $\Delta E = h\nu$

The difference in energy between the two quantum levels of a nucleus with  $I=1/2$  depends on the applied magnetic field  $B_0$  and the magnetic moment  $m$  of the nucleus. The relationship between these energy levels and the frequency  $\nu$  of absorbed radiation is calculated as follows.  $E$  is the expression for a given nuclear energy level in a magnetic field:

$$E = -m \left( \frac{\mu}{I} \frac{h}{2\pi} \right) B_0 = -m \left( \gamma \frac{h}{2\pi} \right) B_0 \quad (29)$$

where  $m$  is the magnetic quantum number;  $m$ , the nuclear magnetic spin;  $B_0$ , the applied magnetic field;  $I$ , the spin angular momentum;  $\gamma$ , the magnetogyric ratio; and  $h$ , Planck's constant.

Equation (29) is the general equation for a given energy level for all nuclei that respond in NMR.

$$\Delta E = h\nu = \frac{\mu}{I} \frac{h}{2\pi} B_0 = \gamma \frac{h}{2\pi} B_0 \quad (30)$$

Therefore, the absorption frequency that can result in a transition of  $\Delta E$  is:  $\nu = \gamma \frac{B_0}{2\pi}$

or  $\omega = \gamma B_0$ , (Larmor equation), which is fundamental to NMR[15]. It indicates that for a given nucleus there is a direct relationship between the frequency  $\omega$  of RF radiation absorbed by that nucleus and the applied magnetic field  $B_0$ . This relationship is the basis of NMR [15, 16].

#### 2.4.2 Spin-spin splitting in proton NMR

Peaks are often split into multiple peaks due to interactions between non equivalent protons on adjacent carbons, called spin-spin splitting. The splitting is into one more peak than the number of H's on the adjacent carbon (“n+1 rule”)

The separation of peaks in a multiplet is measured and is a constant, in Hz [21]; nuclei which are close to one another could cause an influence on each other's effective magnetic field. If the distance between non-equivalent nuclei is less than or equal to three bond lengths, this effect is observable. This is called spin-spin coupling or J coupling. The coupling constant J (in unit of Hertz) is the separation between the two peaks in NMR spectrum. If there are two proton nuclei in a molecule they both are have magnets and influence each other. The magnitude of coupling constant is always the same in the two nuclei that are coupled to each other and it depends only on the

relationship between the two nuclei. And if there are more protons in a molecule, each contributes to the splitting, in a way that one can predict.

### 2.4.3 Chemical Shift

In NMR experiment, proton in different chemical environments within a molecule absorb at slightly different frequencies, this variation, in absorption frequency is caused by a slight difference in the electronic environment of the proton as a result of different chemical bonds and adjacent atoms[15]. The absorption frequency for a given proton depends on the chemical structure of the molecule. This variation in absorption frequency is called chemical shift. Thus, the chemical shift of a nucleus is measured (and defined) the difference between the resonance frequency of the nucleus and a standard, relative to the standard. This quantity is reported in ppm, and given the symbol delta ( $\delta$ ).

$$\delta(\text{ppm}) = \frac{\nu - \nu_{ref}}{\nu_{ref}} \cdot 10^6 \quad (31)$$

For  $^1\text{H}$  NMR spectroscopy tetramethylsilane (TMS), which has a chemical formula  $\text{Si}(\text{CH}_3)_4$ , is well known standard reference. In the TMS all 12 hydrogen nuclei are chemically equivalent, this means that all hydrogen nuclei in the TMS exposed to the same shielding and give a single absorption peak [15]. The chemical shift for other hydrogen nuclei is represented as above Eq. (31).

### 2.4.4 NMR Data Processing

Depending on the chemical environment, there are variations on the magnetic field that the nuclei feel even for the same type of nuclei. The oscillation of the net nuclear magnetization on the xy-plane give a current in a coil, which is the NMR signal and it is detected on xy-plane.

Because the chemical shifts of the peaks in the spectrum are calculated from frequency difference from TMS. This type of spectrum is a frequency-domain spectrum. Peaks generated by a continuous-wave instrument have ringing; a decrease series of oscillations that occurs after the instrument has scanned through the peak. Ringing occurs because the excited nuclei do not have time to relax back to their equilibrium state before the fields of the instrument have advanced to a new position. The excited nuclei have a relaxation rate this is slower than the rate of scan. As a

result, they are still emitting an oscillating, rapidly decaying signal, which is recorded as ringing.

### 2.4.5 The Fourier Transform (FT) NMR

The NMR instrument uses a powerful, but short burst of energy, called a pulse that excites all the magnetic nuclei in the molecule simultaneously.

When the pulse is discontinued, the excited nuclei begin to lose their excitation energy and return to their original spin state, or relax. As each excited nucleus relaxes, it emits electromagnetic radiation. Since the molecule contains many different nuclei, many different frequencies of electromagnetic radiation are emitted simultaneously. This emission is called a free-induction decay (FID) signal (figure 9). The intensity of FID decays with time as all of the nuclei eventually lose their excitation. The FID is superimposed combination of all the frequencies emitted and can be quite complex. We usually extract the individual frequencies due to different nuclei by using a computer and a mathematical method called a Fourier transform (FT) analysis. By computing the Fourier transform of the signal-averaged FID. The usual frequency-domain spectrum can be obtained. The signal-averaged FIDs on the left side of the figure 9 yield the frequency spectra on the right side after Fourier transformation [16, 20].

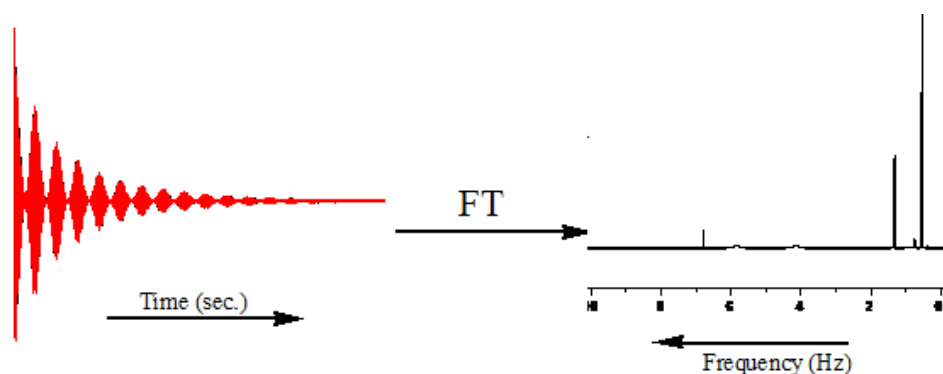


Figure 9. The free induction decay (FID) is on the left and its Fourier transform (usual frequency spectrum) is on the right of an amide

## 2.5 Temperature dependent on rotational barrier of amide bond

### 2.5.1 Evaluation of rate exchange constant (k)

Internal rotational around the amide bond (see figure 5) leads to an intramolecular exchange of  $H_a$  and  $H_b$ . Because of the energy barrier to rotation, it was found that  $H_a$  and  $H_b$  are not equivalent on the NMR time scale. The exchange frequency is low at low temperature. The life time of the exchange of  $H_a$  and  $H_b$  is thus relatively long and consequently two separate signals are observed. If the temperature is raised, these signals broaden and is said to be coalescence temperature, and the temperature is greater than the coalescence a single peak observed. Here the term “chemical shift timescale” is used to express the above conditions. Changes in the appearance of spectra with temperature occur when the rate of exchange becomes comparable to the chemical shift difference between the sites (typically 10-1000Hz), and so the chemical shift timescale is of the order of  $10^{-1}$ - $10^{-3}$  s. the rate of exchange may be slower or faster than this, and varying the temperature at which the NMR spectra dynamic information may be obtained. NMR spectra may thus show the individual components present (slow exchange) or the average site of those nuclei in fast exchange. This situation contrasts with that in IR or UV-Vis spectroscopy where the differences in resonating frequency between different bands are very large ( $10^{12}$ - $10^{14}$  Hz). This is far faster than the rates of chemical reactions (diffusion limits reaction rates to  $10^9$ - $10^{10}$  Hz), and as a result IR and UV-Vis spectra are always in the slow exchange limit, i.e. they show a mixture of all the individual component present.

If two groups chemically equivalent nuclei are exchanged by an intermolecular process, the NMR spectrum is a function of the difference in their resonance frequencies [17],  $\nu_A - \nu_B = \Delta\nu$ , and of the rate and of the rate of exchange, k. (a typical value for  $\Delta\nu$  is about 10Hz.) the effect of exchange at several temperatures on the line width at  $\nu_A$  and  $\nu_B$  are shown in figure 10. At low temperatures the exchange is slow and  $k \ll \Delta\nu$ . The spectrum thus consists of two sharp singlets at  $\nu_A$  and  $\nu_B$  (figure 10. A). at high temperatures the exchange is fast; i.e.  $k \gg \Delta\nu$ , and a single sharp peak is observed (figure 10 D). there is also an intermediate temperature range over which the spectrum consists of two significantly broadened overlapping

lines (figure 10B). Usually spin-spin-lattice relaxation determines the width of an NMR absorption peak. Here we are concerned with the additional effect of exchange of two groups of chemically equivalent nuclei on line width. The Heisenberg uncertainty principle states that the product of the uncertainty in the measurement of the energy of a particular state,  $\Delta E$  and the uncertainty in the lifetime of the state,  $\Delta t$ , is approximately equal to  $\hbar$ ; i.e.

$$\Delta E \Delta t \approx \hbar \quad (32)$$

Since  $\Delta E = h \Delta \nu_{1/2}$  the absorption linewidth,  $\Delta \nu_{1/2}$ , for the transition, is inversely proportional to the lifetime of the excited state

$$\Delta \nu_{1/2} = \frac{\Delta E}{h} = \frac{\Delta E \Delta t}{h \Delta t} = \frac{1}{2\pi \Delta t} \quad (33)$$

An exact analysis of the line broadening produced by the exchange process is derived from the Bloch equations (34). The Bloch equations describe the motion of the bulk magnetic moment of a sample in the presence of a static field,  $H_0$ . And a rotating field,  $H_1$ , perpendicular to  $H_0$ .

The exact function for the lineshape in the case of two equivalent exchanging groups with no coupling is given by

$$g(\nu) = \frac{K\tau(\nu_A - \nu_B)^2}{\left[ \frac{1}{2}(\nu_A - \nu_B) - \nu \right]^2 + 4\pi^2\tau^2(\nu_A - \nu)^2(\nu_B - \nu)^2} \quad (34)$$

Where  $g(\nu)$  is the intensity at frequency,  $\nu$ ;  $K$  is a normalization constant and,  $\tau = 1/k$  where  $k$  is the rate constant for the exchange.  $\tau$ ,  $\nu_A$  and  $\nu_B$  are functions of the temperature and cannot be determined separately. Computer programs are available in which estimated values for  $\tau$ ,  $\nu_A$  and  $\nu_B$  are used to generate  $g(\nu)$ , which is then compared to the experimental spectrum. Values for  $\tau$ ,  $\nu_A$  and  $\nu_B$  are chosen such that the deviation between the experimental and calculated line shapes is minimized. Alternatively various approximations can be made which apply over different ranges of exchange rates.

## 2.5.2 Approximate methods for evaluation of rate constant (k)

Direct calculation of the lifetime of a specific spin state from Eq.(34) can be made over a limited temperature range. Beyond a certain temperature the rate of exchange is so fast that the magnetic environments of the two sets of nuclei are identical and any possible distinction between the two set of nuclei is lost. Thus we have only one set of spins with a lifetime determined by spin-spin and spin-lattice relaxation mechanisms.

As the temperature is varied from values at which the rate of exchange is low enough values of intermediate exchange rates to rapid exchange, a series of approximations is available for the calculation of lifetimes. Although these approximate methods provide somewhat less accurate results than does Eq. (34), it provides a meaningful treatment for the data obtained by NMR of studying kinetic process [17].

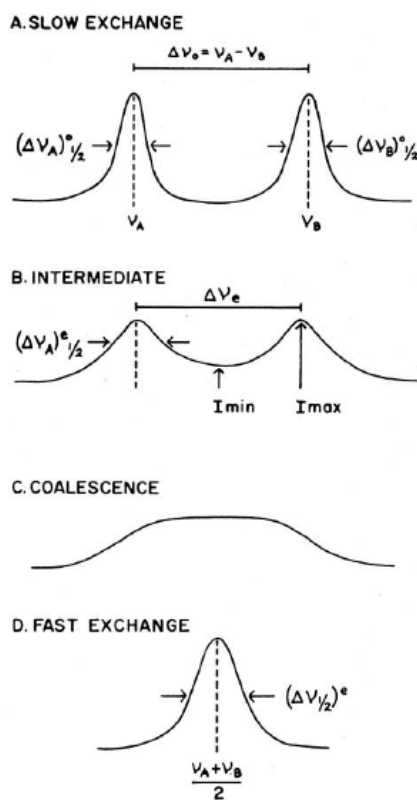


Figure 10. Effect of exchange of chemically equivalent nuclei on NMR lineshapes [17].

At slow exchange rates the spectrum consists of two lines.  $(\Delta v_i)_{1/2}$  it is determined by comparing linewidths at half height of exchanging peaks to those of peaks recorded at temperatures where the rate of exchange is very small

$$k = \pi \left[ (\Delta v_e)_{1/2} - (\Delta v_0)_{1/2} \right] \quad (35)$$

For slow exchange the rate can also be related to the change in peak separation. Eq. (36) applies over the limited range where there is extensive overlap between the two separate peaks (but not too close to coalescence, see below)

$$k = \frac{\pi}{\sqrt{2}} (\Delta v_0^2 - \Delta v_e^2)^{1/2} \quad (36)$$

Where  $\Delta v_i$  is the peak separation in Hz, and the subscripts (i=e or 0) have the previously defined meanings.

A third method applies in the slow exchange region. In the ratio method, k is calculated from the ratio of the intensities of the peaks,  $I_{\max}$ , to the intensity midway

between the peaks,  $I_{\min}$ ,  $r = I_{\max}/I_{\min}$ , and

$$k = \frac{\pi \Delta v_0}{\sqrt{2}} \left( r + (r^2 - 1)^{1/2} \right)^{-1/2} \quad (37)$$

The coalescence temperature is defined as the temperature at which the appearance of the spectrum changes from that of two separate peaks to that of a single, flat-topped peak (see figure 10 C). At this temperature the rate constant can be approximate:

$$k = \frac{\pi \Delta v_0}{\sqrt{2}} \quad (38)$$

At temperatures above the coalescence temperature, the spectrum consists a single peak, i.e., fast exchange. In this region  $\tau \ll (\nu_A - \nu_B)^{-1}$  and Eq. (4) reduces to

$$g(\nu) = \frac{KT_2'}{1 + 4\pi^2 T_2'^2 (\nu_A + \nu_B - 2\nu)^2} \quad (39)$$

With  $1/T_2' = (1/T_{2A}' + 1/T_{2B}')/2$ . The fast exchange limit is sometimes called extreme narrowing. If the signal is not completely collapsed, i.e., the process is slow enough to contribute to its width but still well beyond the rate corresponding to separate signals, the following approximation results [17].

$$k = \frac{\pi \Delta v_0^2}{2} \left[ (\Delta v_e)_{1/2} - (\Delta v_0)_{1/2} \right]^{-1} \quad (40)$$

## 2.6 Temperature dependent of the exchange rate to evaluate thermodynamic quantities

The temperature dependent of the rate constant is used to calculate the activation energy. The relationship between the rate constant at different temperature and activation energy, which is Arrhenius equation, is given by:

$$\ln k = -\frac{E_a}{R} \left( \frac{1}{T} \right) + \ln A \quad (41)$$

Where k=rate constant, A=Arrhenius constant,  $E_a$ =activation energy, R=gas constant, T=absolute temperature. So by plotting  $\ln k$  Vs  $\frac{1}{T}$  the activation energy  $E_a$  can be determined from the slop, i.e., the slop =  $-\frac{E_a}{R}$ , (where  $R = 8.314 \text{ J mol}^{-1} \text{ K}^{-1}$ ).

The Gibbs free energy of activation,  $\Delta G^*$  is also useful for characterizing the transition state of kinetic process,  $\Delta G^*$  is related to the rate constant by Eyring equation

$$k = \left( \frac{k_b T}{h} \right) e^{\Delta G^*/RT} \quad (42)$$

Where k= rate constant,  $k_b$ = Boltzmann's constant, h= Plank's constant,  $\Delta G^*$ =free energy of activation, R= gas constant, T= absolute temperature.

By rearranging the above equation it becomes

$$\Delta G^* = -RT \left[ \ln \left( \frac{k}{T} \right) + \ln \left( \frac{h}{k_b} \right) \right] \quad (43)$$

Since  $\Delta G^* = \Delta H^* - T\Delta S^*$  by combining this with the above equation it gives

$$\ln \left( \frac{k}{T} \right) = -\frac{\Delta H^*}{RT} + \left[ \frac{\Delta S^*}{R} - \ln \left( \frac{h}{k_b} \right) \right] \quad (44)$$

So an Eyring plot of  $\ln\left(\frac{k}{T}\right)$  Versus  $\frac{1}{T}$  give a straight line for which,  $\Delta H^* = -(\text{slope})R$ , and the Y-intercept is  $\frac{\Delta S^*}{R} + \ln \frac{k_b}{h} = \frac{\Delta S^*}{R} + 23.76$  ), and it is used to determine  $\Delta S^*$ , but normally a large extrapolation from the experimental data. Therefore if the linear fit of  $\ln\left(\frac{k}{T}\right)$  versus  $1/T$  is not extremely good, the error in  $\Delta S^*$  can be quite large.

$\Delta G^*$  Can be obtained directly at the coalescence temperature using the formula given below [18].

To calculate  $\Delta G^*$  at each temperature:

$$\Delta G^* = RT \left[ \ln \left( \frac{k_b T}{h} \right) - \ln k_{rate} \right] \quad (45)$$

$\Delta G^* = RT [23.76 - \ln k_{rate}]$ , use  $R=1.9872$  for calories/mol. And  $R = 8.3144$  for joule/mol.

This has been converted a different form using base-10 logarithms

$$\Delta G^* = aT \left[ 10.319 + \log \left( \frac{T}{k_{rate}} \right) \right] \quad (46)$$

Where  $a = 4.575 \times 10^{-3}$  for units of Kcal/mol, and  $a = 1.914 \times 10^{-2}$  for units of KJ/mol [18].

## **3 Objectives**

### **3.1 General objective**

To investigate rotational barrier of nicotinamide and picolinamide at variable temperatures using  $^1\text{H}$  NMR spectroscopy.

### **3.2 Specific objectives**

The specific objectives of this study include investigation and

- Determine the temperature dependent of the proton NMR absorption peaks of the nicotinamide and picolinamid.
- Determination of the magnitude of the kinetic and thermodynamic parameters for rotational barrier of nicotinamide and picolinamide.
- Comparison of the experimental energy of rotational barrier of nicotinamide and picolinamide with theoretical values.
- Suggest the tautomeric structure of the nicotinamide and picolinamide in a solution.

## 4 Experimental part

### 4.1 Materials

Nicotinamide (BDH, laboratory reagent, England) Picolinamide (98% Alfa Aldrich Japan), the solvent deuterated benzene (99.5%, Fluca-Garantie, Switzerland), and the solvent ACN (99.9%, Sigma-Aldrich, Switzerland), and carbon tetrachloride ( $\text{CCl}_4$ ) in 2% tetramethylsilane (TMS) used for proton NMR measurements. Distilled water and Acetone (99.9%, Sigma-Aldrich, Switzerland) were used as cleaning agents. All the above chemicals were studied without further purifications.

### 4.2 Methods and procedures

#### 4.2.1 Proton NMR measurements

Proton NMR spectra of nicotinamide and picolinamide solutions were recorded with a Bruker Avance 400 MHz spectrophotometer. The typical spectral conditions were as follows: Acquisition time 2 second and 4 scans per spectrum. The spectra were acquired over a range of 298 K–333 K for nicotinamide and 296 K–336 K for picolinamide in ACN solvent and 296 K–338 K in  $\text{C}_6\text{D}_6$  through a Bruker Avance digital variable-temperature control unit.

Small amount of nicotinamide was taken and dissolved in ACN solvent, and small amount of picolinamide in ACN and duterated benzene with different beaker are also dissolved.

The samples are transferred to a clean and dry NMR tube degassed and permanently sealed. Degassed is required in order to remove paramagnetic oxygen which, if not removed, would result in an additional indeterminate line broadening factor. Spectrum of these solutions were recorded in carbon tetrachloride containing 2% TMS.

Any NMR spectrometer equipped with a variable temperature probe may be used for the spectral measurements. A series of spectra is recorded at each temperature until no further change in spectral characteristics (line-width or peak separation) is observed. The resolution of the instrument should be checked at each temperature by recording the methyl resonance of TMS. The data are divided into three groups corresponding to

slow exchange and intermediate exchange, coalescence temperature and fast exchange.

After the NMR data Fourier transformed into ASCII file using MestReC software, and origin software which is used to plot the spectrum, exact line position and line-widths are extracted to determine the exchange rate and the Arrhenius plot ( $\ln k$  Vs  $1/T$ ) is used to calculate the activation energy, and the Eyring plot ( $\ln(k/T)$  Vs  $1/T$ ) is used to calculate the enthalpy change and entropy change. And plotting the frequency versus temperature to see the trend clearly in the  $^1\text{H}$  NMR spectra of the amide.

## 5 Results and Discussion

### 5.1 $^1\text{H}$ NMR Result Nicotinamide

The resonance structure causes C-N partial double bond of 1<sup>st</sup> order amides, nicotinamide is presented, the two protons of amine group of the amide were detected and they are on the different chemical shifts of the  $^1\text{H}$  NMR spectra, and energy is required to rotate about the C-N partial double bond of amides. The effect of the rotational barrier depend on temperature; i.e. under the condition of low temperatures different magnetic environments for the two protons on nitrogen of the amide, give two peaks of equal intensity (figure 10) which is slow rotation about the amide bond, and vanish at high temperatures. At coalescence temperature broadening peak is detected, which implies that the two protons on the amine of the amide are broadly overlapping.

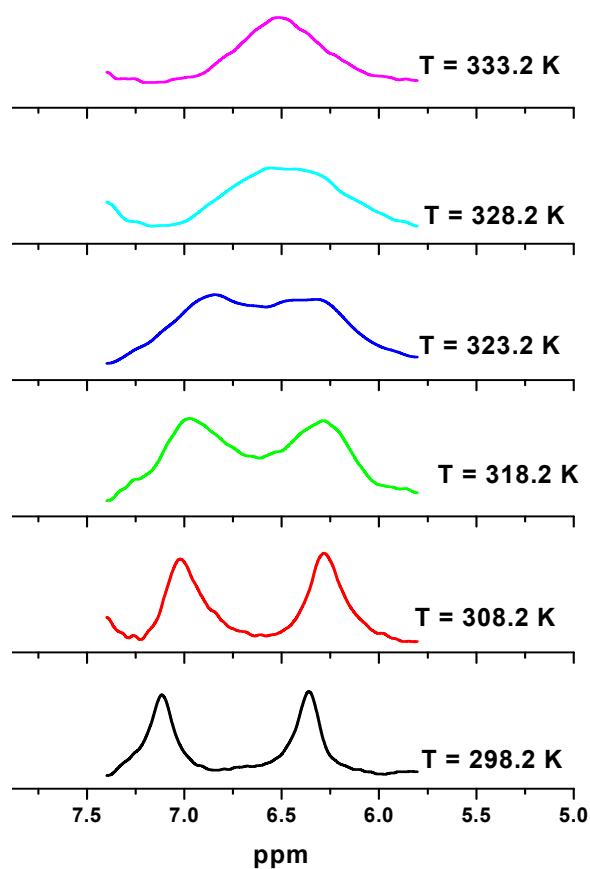


Figure 11. Effect of temperature on lineshape for the two protons on nitrogen in nicotinamide in ACN.

The above figure shows the proton NMR spectra of nicotinamide at variable temperatures the coalescence temperature was detected at 328 K. At temperatures below the coalescence temperature few molecules have sufficient energy to overcome the barrier to rotation. However, at temperatures greater than the coalescence temperature, many molecules have sufficient thermal energy to overcome the barrier and therefore rotation occurs [19]. And at high temperature, greater than the coalescence temperature, the rotation about the amide bond is fast, which implies that the two protons on nitrogen of the amide peaks are collapse to a single peak. The environments of protons on nitrogen of the amide, in the pair of rotamers are identical. Thus the spectrum is the single line characteristic of free rotation about a single bond. Further increases in temperature cause the line to narrow.

## 5.2 Determination of Kinetic Parameter for Nicotinamide

### 5.2.1 Rate exchange constant (k)

The exchange rate constant can be calculated using change of peak separation and change of peak width of the proton NMR spectra of the two protons on the nitrogen of the amide, and are listed below the table.

Table 1. Change of peak separation and peak widths at half height with various temperatures of nicotinamide

Temperature(K)	Peak separation( $\Delta\nu$ )/Hz
298.2	0.755
308.2	0.741
318.2	0.684
323.2	0.456
328.2	0
333.2	$(\Delta\nu_e)_{1/2} = 0.461\text{Hz}$
	$(\Delta\nu_o)_{1/2} = 0.137\text{Hz}$

At a temperature of 308.2 K, the rate constant can be determined using equation (35)

$$\text{which is } k = \frac{\pi}{\sqrt{2}} (\Delta\nu_o^2 - \Delta\nu_e^2)^{1/2}$$

$$k = \frac{\pi}{\sqrt{2}} \left( (0.755\text{Hz})^2 - (0.741\text{Hz})^2 \right)^{1/2} = 0.321\text{Hz}$$

At a temperature of 318.2K,  $k = \frac{\pi}{\sqrt{2}} \left( (0.755\text{Hz})^2 - (0.684\text{Hz})^2 \right)^{1/2} = 0.710\text{Hz}$

At a temperature of 323.2 K,  $k = \frac{\pi}{\sqrt{2}} \left( (0.755\text{Hz})^2 - (0.456\text{Hz})^2 \right)^{1/2} = 1.337\text{Hz}$

At coalescence temperature which is 328.2 K, the rate constant (k) determined by using the equation (38)  $k = \frac{\pi\Delta\nu_0}{\sqrt{2}}$

$$k = \frac{\pi(0.755\text{Hz})}{\sqrt{2}} = 1.677\text{Hz}$$

For fast exchange at a temperature of 333.2 K, the rate constant (k) determined by equation (40)

$$k = \frac{\pi\Delta\nu_0^2}{2} \left[ (\Delta\nu_e)_{1/2} - (\Delta\nu_0)_{1/2} \right]^{-1}$$

$$k = \frac{\pi(0.755\text{Hz})^2}{2} [0.461\text{Hz} - 0.137\text{Hz}]^{-1} = 2.764\text{Hz}$$

Table 2. Typical value for  $k_{\text{rate}}$  for nicotinlamide

Temperature (K)	$K_{\text{rate}} (\text{s}^{-1})$
298.2	---
308.2	0.321
318.2	0.710
323.2	1.337
328.2	1.677
333.2	2.764

The rate of exchange between the two magnetic environments increases as the temperature is increased.

### 5.2.2 Activation energy

After the temperature dependence of the rate constants are obtained, we can calculate the activation energy, using Eq. (41) which relates the rate constant at different temperature and activation energy

$$\ln k = -\frac{E_a}{R} \left( \frac{1}{T} \right) + \ln A$$

So  $\ln k$  Vs  $\frac{1}{T}$  can be plotted and giving a straight line with the slope  $= -\frac{E_a}{R}$ , (where  $R = 1.987 \text{ cal mol}^{-1} \text{ K}^{-1}$ )

So in this experiment the activation energy is found to be  $17.948 \text{ Kcal mol}^{-1} \text{ K}^{-1}$  (see appendix A)

## 5.3 Determination of Thermodynamic Parameters for Nicotinamide

### 5.3.1 Enthalpy change, entropy change, and free energy change

From rate exchange constant at variable temperatures in the Eyring equation (Eq.44) which can be used to determine  $\Delta H$ ,  $\Delta S$  and  $\Delta G$ .

$$\ln \left( \frac{k}{T} \right) = -\frac{\Delta H^*}{RT} + \left[ \frac{\Delta S^*}{R} - \ln \left( \frac{h}{k_b} \right) \right]$$

So an Eyring plot of  $\ln \left( \frac{k}{T} \right)$  versus  $\frac{1}{T}$  give a straight line (see Appendix B)

For which,  $\Delta H^* = -(\text{slope})R$ .

$$\Delta H^* = -(-8496.552)1.987 \text{ cal K}^{-1} \text{ mol}^{-1} = 16.883 \text{ Kcal K}^{-1} \text{ mol}^{-1}$$

And the Y-intercept =  $\frac{\Delta S^*}{R} + \ln \frac{k_b}{h} = \frac{\Delta S^*}{R} + 23.76$  , and it is used to determine  $\Delta S^*$  ,

At the coalescence temperature  $\Delta S^* = -6.11 \text{ kcal.mol}^{-1}$

The significant of  $\Delta S^*$  : large positive value indicates less ordered transition state

Large negative value indicates more ordered transition state. Here the small negative value of entropy change somewhat ordered transition state indicated.

Using The Eyring equation, Eq. (46),  $\Delta G^*$  can be calculated at coalescence temperature. (Note that  $\Delta S^*$  is usually  $\ll \Delta H$  , so the temperature dependence of  $\Delta G^*$  is usually undetectable within error)

$$\Delta G^* = aT \left[ 10.319 + \log \left( \frac{T}{k_{rate}} \right) \right]$$

$$\Delta G_{308.2}^* = 4.575 \times 10^{-3} (308.2) \left[ 10.319 + \log \left( \frac{308.2}{0.321} \right) \right] = 18.755 \text{ Kcal.mol}^{-1}$$

Table 3. Comparison of Experimental energies for rotational barrier of nicotinamide

sample		$\Delta H$ (Kcal mol <sup>-1</sup> )	$\Delta S$ (cal mol <sup>-1</sup> )	$\Delta G_{308.2 \text{ K}}$ (Kcal mol <sup>-1</sup> )	Ref.
nicotinamide	experimental	16.9	-6.1	18.7	This work
	From computational <sup>(a)</sup>	12.9±0.3	-7.7±0.9	15.3	23

<sup>(a)</sup> The structures optimized at HF/6-31G(d,p). Corrected with zero point energies at HF/6-31G(d,p) in nitrobenzene solvent.

The experimental results obtained in this work were in a good agreement with the theoretical values.

## 5.4 The $^1\text{H}$ NMR Result for Picolinamide

The  $^1\text{H}$  NMR study of picolinamide in ACN and benzene solvents at variable temperatures (figure 12) shows the effect of the two magnetically non-equivalent protons on the nitrogen of the amide. The two protons on the nitrogen of the amide are denoted by asterisks.

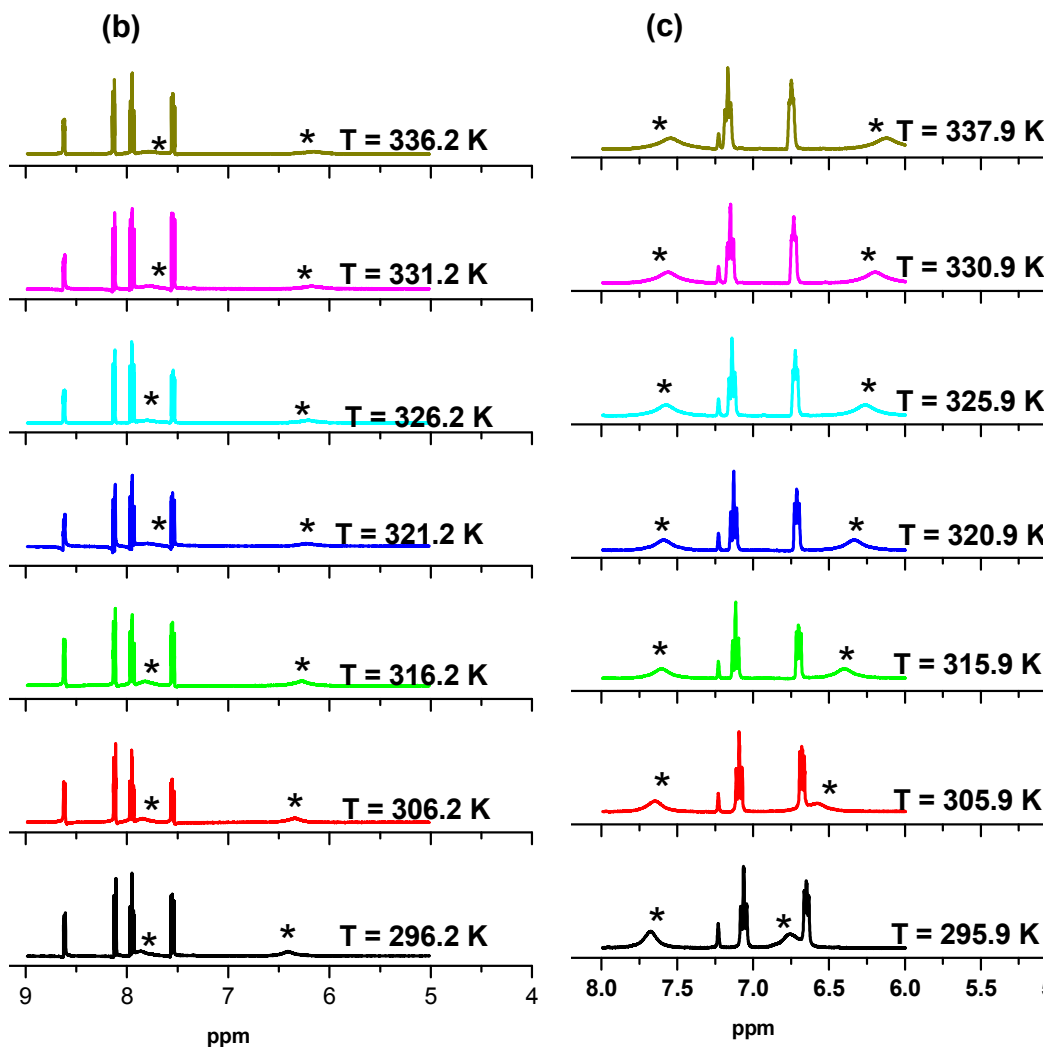


Figure 12. the proton NMR spectra of picolinamide (b) in acetonitrile and (c) in benzene solvents as a function of temperature.

Plotting chemical shift of peak separation versus temperature gives straight line (see figure 12,13, and 14)

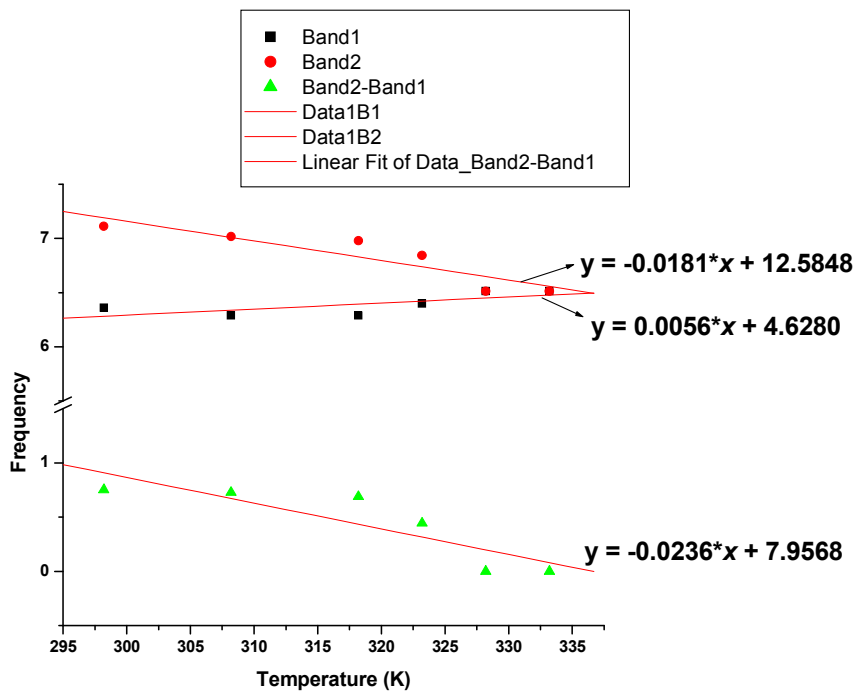


Figure 13. Plot of frequency versus temperature of nicotinamide in acetonitrile

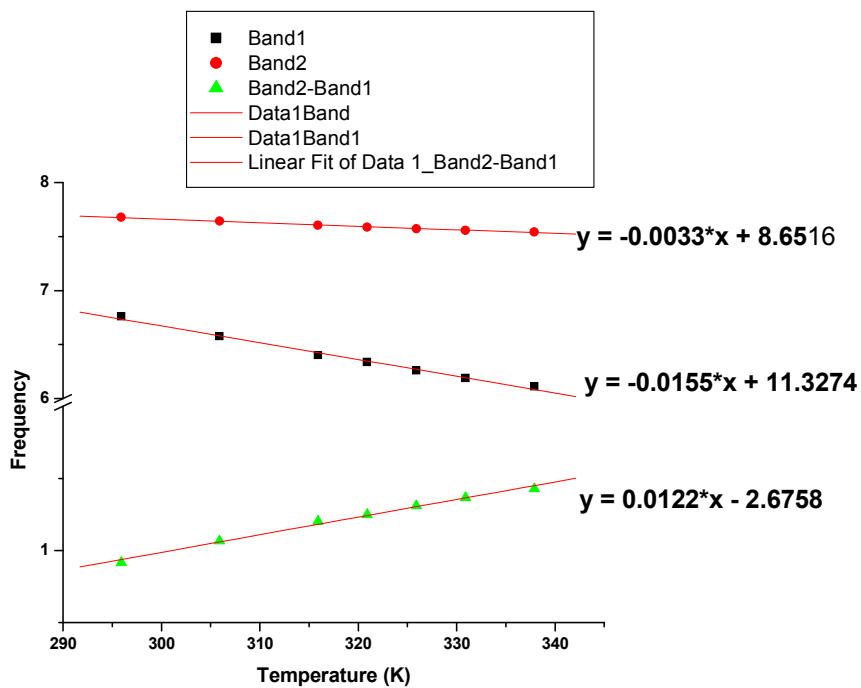


Figure 14. plot of frequency versus temperature of picolinamide in benzene

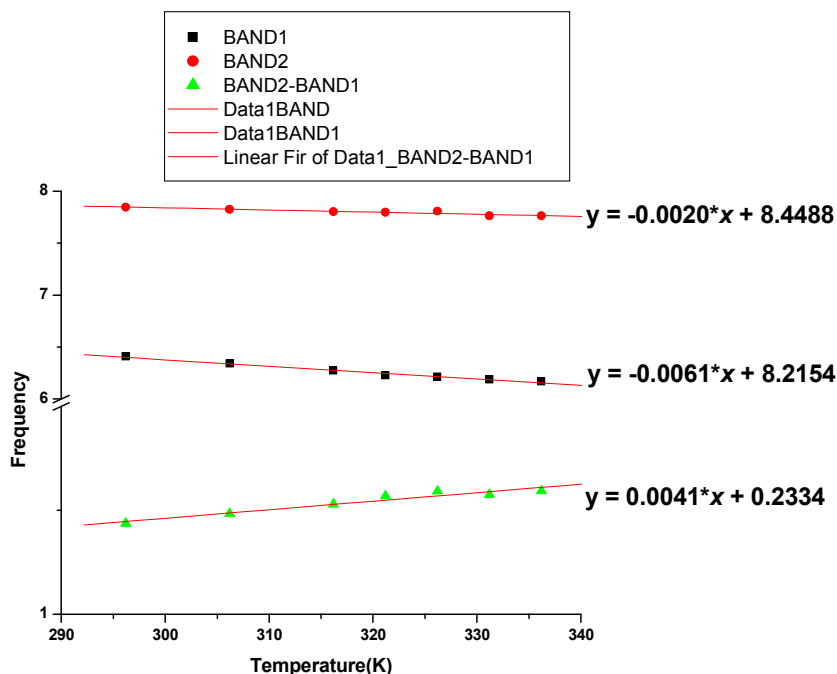


Figure 15. plot of frequency versus temperature of picolinamide in Acetonitrile

For Nicotinamide (figure 13) as it is clearly seen the slope of the peak separation is negative so it implies that the band1 and band 2 are converge i.e., at some point the two bands coalesce, and this implies that there is rotational on the amide bond of nicotinamide. while in the picolinamide in both solvents the slope of peak separation are positives (figure 14 and 15), i.e., the peak separation increasing as temperature increase so the band1 and band2 do not converge, this implies that there is no rotation about the C–N bond of picolinamide.

So here are the suggestions, Since nicotinamide showed two distinct peaks corresponding to the two magnetically non equivalent protons of the amine group in the amide molecule at room temperature (figure 16)

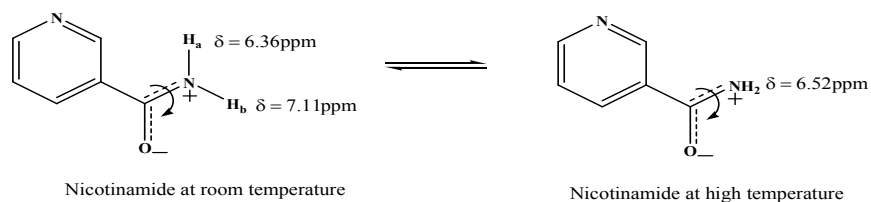


Figure 16. The chemical shifts of nicotinamide at different temperatures.

and at high temperature, due to a rapid rotation about the C–N bond of the amide the magnetic non-equivalence of the protons disappear, therefore only a single peak be observed in the proton NMR spectra (figure 16)

And the picolinamide the two bands are suggested as O–H and =N–H at high temperatures, due to the formation of imidic acid tautomers are favourable at high temperatures. And therefore the peaks of the two protons of are chemically different as shown in the figure 17.

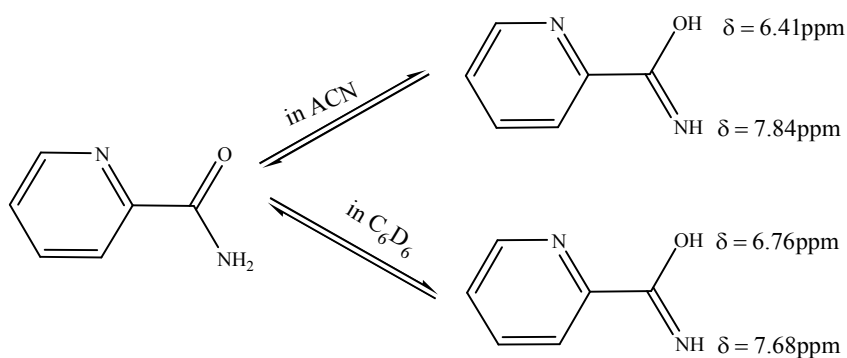


Figure 17. the chemical shifts of the tautomeric form of picolinamide

## 6 Conclusion

In this work, investigation of rotational barrier in nicotinamide and picolinamide at various temperatures using proton NMR spectroscopy were studied. In nicotinamide two distinct peaks from protons of amine group of the amide molecules, the separation of these peaks decreased as a function of temperature indicating a rotational barrier about the amide bond. The coalescence of the two peaks was observed at 328 K. Using through line shape analysis of the temperature dependent spectra; a rotational barrier of  $17.9 \text{ kcal mol}^{-1}$  was calculated.

However in the picolinamide at high temperatures the two distinct peaks suggested as the protons of imidic acid tautomeric form of the amide i.e., of O-H, and =N-H. These two peaks do not converge as a function of temperature; this implies that there is no rotation about the amide bond.

## 7 References

1. L. Wang, C. T. Middleton, M. T. Zanni, and J. L. Skinner, *J. Phys. Chem., B*, 2011, 115(13): 3713–3724.
2. A. Borba, A. Gomez-Zavaglia, and R. Fausto. *J. Phys. Chem., A*, 2008, 112, 45-57.
3. Quintanilla-Licea R., Juan F. Colunga-Valladares, Caballero-Quintero A., "NMR Detection of Isomers Arising from Restricted Rotation of C-N Amide bond of N-Formyl-o-toluidine and N,N'-bis-Formyl-o-toluidine" *Molecules August 2002*, 7, 662-673.
4. Clayden, Greeves, Warren, and Wothers "Organic Chemistry" USA, Oxford University 2001.
5. Kenneth B. Wiberg and Curt M. Breneman "Resonance Interactions in Acyclic Systems, Formamide Internal Rotation Revised, Charge and Energy Redistribution along the C-N Bond Rotational Pathway" New Haven, 1991.
6. M. Horwath, V. Benin. "C-N Bond Rotation and E-Z Isomerism in Some N-Benzyl-N-Methylcarbamoyl Chloride: A DFT Study" 2007.
7. L. D Field, S. Sternhell, J.R. Kalman "Organic Structures from spectra" 2008, 4<sup>th</sup> ed.1-2.
8. M. Hailu, "Investigation of solvent Effects on N-H Stretching Vibrational Frequency of propylamide", MSc Thesis, AAU, 2013
9. Ira N. Levine "Physical Chemistry", 6<sup>th</sup> ed., New York, 2009 .
10. M. G. Papadopoulos, A. J. Sadlej and J. Leszczynski, "Non-Linear Optical Properties of Matter" (2006), Springer.
11. A. Wolski, "Theory of Electromagnetic Fields", University of Liverpool and the Cockcroft Institute, UK.
12. R. Cammi, B. Mennucci and J. Tomasi, *J. Phys. Chem., A*, (2000), 4690-4698.
13. R. Wortmann and D. M. Bishop, *J. Chem. Phys.*, (1998), 108(3), 1001-1007.
14. J. J. Wolff, R. Wortmann *Adv. in Phy. Org. Chem.* Vol.32 121-161.1999.
15. J. W. Robinson, E. M. Skelly Frame "undergraduate instrumental analysis" 2005, 6<sup>th</sup> ed. New York, USA.
16. D. L. Pavia, G. M. Lampman, G. S. Kriz, J. R. Vyvyan. "Introduction to spectroscopy", 2009, 4<sup>th</sup> ed.

17. F. P. Gasparro, N. H. Kolodny, “*NMR Determination of Rotational Barrier in N,N-dimethylacetamide.*” 2011.
18. Zimmer, R. Shoemaker, Ruminski , *Inorganica Chimica Acta*, 2006. 1478-1484.
19. M. Rabinovitz, A. Pines, “*Hindered Internal Rotation and Dimerization of N,N-Dimethylformamide in Carbontetrachloride*”,1968 .
20. T. L. James “*Fundamentals od NMR*” 1998, San Francisco, USA
21. J. McMurry, “*Organic Chemistry*”, 2008, 7<sup>th</sup> ed. Physical. Sciences.
22. Yisak Tsegazab “*Structural and Dimerization Analysis of Some Primary Amides*” Msc Thesis. AAU. 2014.
23. Ryan A. Olsen, Lisa Liu, Nima Ghaderi,Adam Johns,Mary E. Hatcher,and Leonard J. Mueller “*The Amide Rotational Barriers in Picolinamide and Nicotinamide: NMR and ab Initio Studies*” 2002.

## 8 Appendices

### Appendix A.

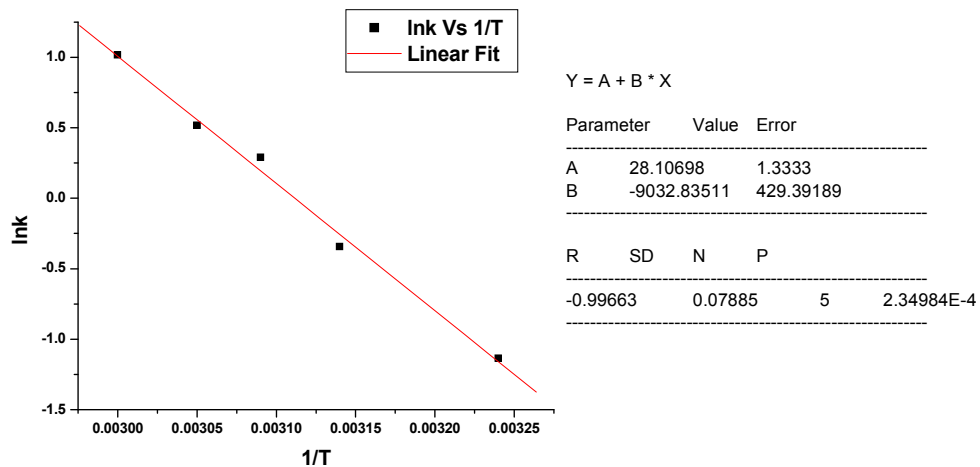


Figure 18. ln k Vs 1/T for nicotinamide

### Appendix B.

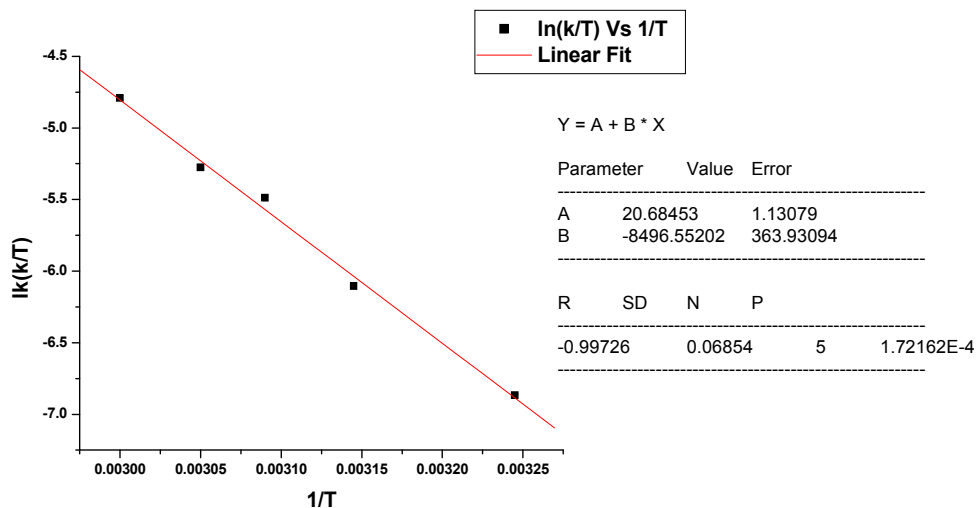


Figure 19. ln(k/T) Vs 1/T for nicotinamide.